LUNAR CRATERS AND SOILS: AGES, COLORS, AND REGOLITH THICKNESSES; A.S. McEwen, L.R. Gaddis, USGS, Flagstaff, AZ; G. Neukum, H. Hoffmann, DLR, Berlin, Germany; C.M. Pieters, J.W. Head III, Brown University, Providence, RI.

The spectral reflectivities of lunar soils are controlled by (1) the mineralogy of the underlying bedrock, (2) the cumulative age of exposure to the space environment, and (3) vertical and horizonal regolith mixing from impact ejecta. Quantitative regolith evolution models that adequately account for all three contributions listed above could enable accurate dating of relatively recent lunar geologic events, primarily impacts over the past ~1 b.y., from remote multispectral observations. We have quantitatively related multispectral measurements of lunar soils to exposure ages, geologic emplacement ages, and regolith thickness variations. We used three datasets: (1) Galileo Solid-State Imaging (SSI) multispectral observations of the Moon's west nearside and farside; (2) new measurements of the frequencies of craters superposed on the floors and/or continuous ejecta blankets of larger craters, extending the original results of Neukum and Konig (1); and (3) previously published measurements of spectral reflectivity, soil maturity (various parameters), and other information on the returned samples of lunar soils.

Most soil evolution models are based on the scenario described by McKay et al. (2). As micrometeorites bombard the lunar surface, soil grains are comminuted and black agglutinates are formed from the fine dust component by melting and agglomeration. Larger impacts excavate fresh subsurface material that buries or is mixed with nearby soils. With continued surface exposure and small-scale impact "gardening," a steady "mature" state may be reached in which the mean grain size and agglutinate content do not change until interrupted by a rare larger impact that buries the soil and resets the surface exposure age. An impact that excavates to depths much greater than the regolith thickness will emplace crater floor materials and continuous ejecta with exposure ages near zero. The buried soil may be reexcavated by a subsequent event and returned to the surface to undergo further maturation. In addition to small-scale impact gardening, which may be thought of as "in situ" processing, and large nearby events that reset the soil exposure age, medium-sized or large distant impacts will contribute "outside" materials that are mixed into the soil. In regions of thin regolith, this outside contribution will be dominated by fresh crystalline materials, whereas regions of thick regolith will contain a greater proportion of soils with a non-zero exposure history.

We have examined the multispectral data and superposed crater frequencies of large isolated craters, mostly of Eratosthenian and Copernican ages, to avoid complications due to secondaries (as they affect superposed crater counts) and to spatially nonuniform regolith mixing from other nearby, large, and younger impacts (as it affects regolith evolution models). The new crater size-frequency measurements refine and extend the results of (1); our total dataset for the region of the Moon imaged by Galileo includes 11 mare craters and 9 highlands craters (Table 1). Our crater counts indicate that the large craters Hausen (lat -65°, long 88°W; 170 km diameter) and Pythagoras (lat 63°, long 62°W; 120 km diameter) should be reclassified from Eratosthenian to Upper Imbrian; these are additional examples (cf. ref. 1) of how photogeologic crater classification tends to assign younger ages to larger craters.

Correlations are demonstrated between log N (cumulative crater frequency per km^2 reduced to diameter, D = 1 km) and the 0.56/1 micron color ratios and 0.56-micron normal albedos of the crater materials (Table 1). The trends (Fig. 1) are clearly significant for craters younger than Copernicus, but the albedos and colors become saturated for older craters. These results allow estimation of the geologic emplacement age of many other nearside and farside Copernican craters. The linear trends between N and 0.56/1 micron ratio differ between mare and highlands and between the interiors and continuous ejecta of the craters (Fig. 1). Similar trends are established for color and albedo versus soil maturity indices for the returned lunar samples, again with distinct trends for mare and highlands soils. However, the mare versus highland offsets (between trend lines) are reversed in the two comparisons: any particular 0.56/1 micron ratio value corresponds to both a smaller N (younger emplacement age) and a larger maturity index (older exposure age) for highlands craters relative to mare craters. These highlands versus mare crater trends can be explained by variations in regolith thickness and rates of mixing with relatively fresh (immature) ejecta: the soil maturity trends and parameters represent longer geologic time periods for samples over thinner regoliths such as those in the maria, and they represent shorter geologic time periods over the thicker regolith of the highlands. We will use these results to estimate the previously unconstrained rate constants for replenishment by fresh additional materials in regolith evolution models (e.g., 3).

REFERENCES: (1) Neukum, G., and B. Konig, 1976, PLPSC 7, 2867-2881. (2) McKay, D. S., R. M. Fruland, and G. H. Heiken, 1974, PLSC 5, 887-906. (3) Mendell, W. W., and D. S. McKay, 1975, The Moon 13, 285-292. (4) Neukum, G., B. Konig, and J. Arkani-Hamed, 1975, The Moon 12, 201-229.

Table 1. Lunar Crater Data

CRATER	ABBREV-IATION	CUM.[1] N(D=1)	AGE (by)[2] A	AGE (by)[2] B	GRN ALBEDO I[3]	GRN ALBEDO CE[3]	GRN/968 I	GRN/968 CE	DIAMETER (KM)	LAT,LONG (DEG.)
HIGHLANDS[4]:										
Hell Q	HEL	<0.8E-04	<0.10	<0.11	0.27	0.24	0.96	0.88	4	33 S, 4 W
Tycho	TYC	0.80E-04	0.10	0.11	0.26	0.18	0.89	0.78	85	43 S, 11 W
Olbers A	OLB	0.42E-03	0.54	0.50	0.23	0.19	0.89	0.80	43	8 N, 78 W
Philolaus	PHI	0.80E-03	1.02	0.95	0.22	0.20	0.80	0.77	72	72 N, 34 W
Copernicus	COP	0.13E-02	1.66	1.55	0.16	0.11	0.74	0.75	93	10 N, 20 W
Zucchius	ZUC	0.13E-02	1.66	1.55	0.19	0.17	0.84	0.76	65	61 S, 50 W
Carpenter	CAR	0.14E-02	1.79	1.67	0.18	0.17	0.73	0.72	64	69 N, 51 W
Hausen	HAU	0.65E-02	3.6	3.59	0.17	0.16	0.74	0.76	167	66 S, 88 W
Pythagoras	PYG	0.67E-02	3.6	3.60	0.18	0.17	0.75	0.75	130	64 N, 63 W
MARIA:										
Aristarchus	ARI	0.15E-03	0.19	0.18	0.21	0.10	1.00	0.83	40	24 N, 47 W
Kepler	KEP	0.67E-03	0.86	0.80	0.14	0.11	0.85	0.81	32	8 N, 38 W
Diophontus	DIO	0.11E-02	1.41	1.31	0.11	0.11	0.92	0.82	18	28 N, 34 W
Flamsteed	FLA	0.14E-02	1.79	1.67	--	0.09	--	0.83	21	5 S, 44 W
Delisle	DEL	0.15E-02	1.92	1.79	0.10	0.09	0.83	0.77	25	30 N, 35 W
Euler	EUL	0.22E-02	2.82	2.62	0.09	0.07	0.76	0.75	28	23 N, 29 W
Eratosthenes	ERA	0.25E-02	3.2	2.94	--	--	--	--	58	15 N, 11 W
Harpalus	HAR	0.26E-02	3.3	3.00	0.13	0.12	0.80	0.78	35	53 N, 43 W
Timocharus	TIM	0.30E-02	3.4	3.23	0.08	0.08	0.78	0.75	34	27 N, 13 W
Lambert	LAM	0.50E-02	3.5	3.51	0.08	0.08	0.77	0.76	30	26 N, 21 W
Bullialdus	BUL	0.70E-02	3.6	3.61	0.12	0.10	0.79	0.75	61	21 S, 22 W

1. Cumulative crater frequency N (km^{-2}) reduced to diameter = 1 km (see ref. 4). New crater counts were acquired for this paper of the craters Flamsteed, Aristarchus, Copernicus, Kepler, Hausen, Philolous, Carpenter, Olbers A, Pythagoras, Harpalus, and Zucchius. Hell Q is superposed on a ray of Tycho, so its cumulative crater count and age must be less than that of Tycho. Data for other craters are from (1).
2. Age model A is based on assumed constant cratering during past 3.2 b.y; model B is from numerical solution of
$N(D=1) = 5.44 \times 10^{-14} (e^{6.93t} - 1) + 8.38 \times 10^{-4} \times t$, where t is time in billion years.
3. I denotes crater interior and CE denotes continuous ejecta. No I values are given for Flamsteed as the interior was flooded by mare lava. No spectral values are given for Eratosthenes because of apparent contamination by ejecta and rays from Copernicus. Bullialdus may also be contaminated by a ray from Tycho.
4. Copernicus occurs in a region of maria, but it excavated highlands materials, so it is classified here as a highlands crater with respect to its spectral properties.

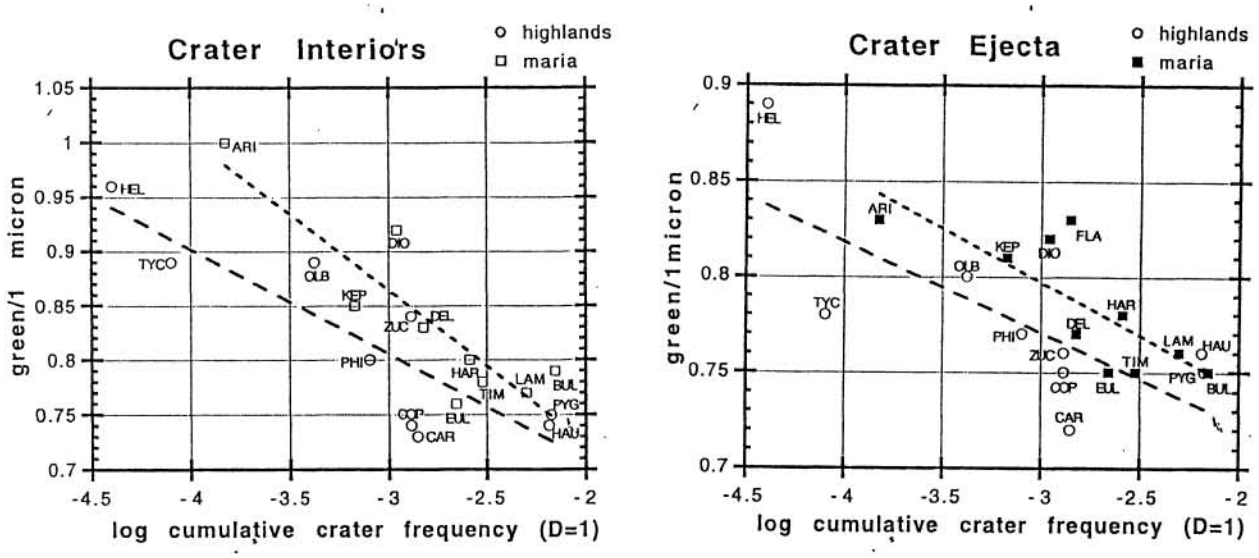

Figure 1. Plots of green/1 micron color ratios versus cumulative crater frequency normalized to a diameter of 1 km (4) for crater interiors (left) and continuous crater ejecta (right).